

Marie Johansson · Jan Nyström · Micael Öhman

Prediction of longitudinal shrinkage and bow in Norway spruce studs using scanning techniques

Received: April 10, 2002 / Accepted: August 21, 2002

Abstract Straightness is one of the most important properties for making timber an attractive material for modern mechanized building. Several studies have shown that a lack of straightness is one of the main reasons for choosing materials other than timber in the construction industry. This paper presents a way to model moisture-induced bow from longitudinal shrinkage data predicted from an analysis of images of the surface of Norway spruce studs. For this study, eight studs ($45 \times 95 \times 2500$ mm and $45 \times 120 \times 3000$ mm) of Norway spruce timber were selected. Bow in these studs was measured at two moisture contents below the fiber saturation point. The studs were then split into three slices 11 mm thick, and the surfaces of these slices were scanned to obtain color information and images of the tracheid effect. The slices were cut into sticks with dimensions of $10 \times 10 \times 200$ mm. The longitudinal shrinkage coefficient of these sticks was measured. A multivariate model was created to model the longitudinal shrinkage coefficient data from the information in the images. The predicted longitudinal shrinkage data was used to model bow. The mean value of the measured longitudinal shrinkage was 0.0121 (SD 0.0123). The root mean square error of prediction (RMSEP) for the multivariate model was 0.0079, which is regarded as good. Thus, it was possible to model moisture-induced bow with good accuracy using the predicted longitudinal shrinkage data.

Key words Color · Tracheid effect · Compression wood · Distortion

M. Johansson (✉)
Department of Structural Engineering, Steel and Timber Structures,
Chalmers University of Technology, SE-412 96 Gothenburg, Sweden
Tel. +46-31-772-2028; Fax +46-31-772-2260
e-mail: marie.johansson@ste.chalmers.se

J. Nyström · M. Öhman
Division of Wood Technology, Luleå University of Technology,
SE-931 87 Skellefteå, Sweden

Introduction

Background

Straightness is one of the most important properties that needs to be enhanced to make timber an attractive material for use in modern mechanized building. Several studies have shown that a lack of straightness is one of the main reasons for choosing materials other than timber in the construction industry.^{1–3} Distortion in the form of twist is caused by large annual ring curvature in combination with spiral grain angle and shrinkage.^{4,5} Bow and spring, on the other hand, are caused mainly by two things: the release of residual stress during sawing^{6,7} and uneven longitudinal shrinkage.^{8,9}

The longitudinal shrinkage may be regarded as small and of no importance for the utilization of timber. The longitudinal shrinkage coefficient α_l (shrinkage per percentage change in the moisture content) for Norway spruce (*Picea abies*) timber is normally about 0.009. This could perhaps be regarded as a low figure, as it only shortens a 3 m long stud by 2.7 mm in conjunction with a change in moisture content from 20% to 10%. However, only a small variation in the longitudinal shrinkage is enough to cause bow and spring in a stud.^{9,10}

Longitudinal shrinkage is a property that varies greatly within one piece of timber. Results have shown that, within the same log, the longitudinal shrinkage coefficient can vary from 0.001 to 0.035.¹¹ A nondestructive method for detecting variations in longitudinal shrinkage would be a valuable instrument for predicting the studs that will develop large bow and spring after drying.

It is well known that some “types” of wood have larger longitudinal shrinkage than “normal” wood. Juvenile wood, compression wood, and fiber deviations around knots are some wood “types” that often display more longitudinal shrinkage than “normal” wood.^{11–14}

Compression wood is a feature of softwood that is difficult to detect, although a few methods have been described. Color information from an imaging spectrometer or an

RGB (red-green-blue) color camera can be used in combination with multivariate calibration to distinguish compression wood from normal wood.^{15,16} The ability of wood fibers to transmit light, often called the tracheid effect, can also indicate the presence of compression wood. The tracheid effect is affected by fiber orientation and potentially also by the presence of juvenile wood.¹⁷⁻²⁰ Modeling longitudinal shrinkage using data from color and tracheid effect scanning may therefore be possible.

Objectives

This study is a joint project between Luleå University of Technology and Chalmers University of Technology. Luleå University of Technology was responsible for the scanning techniques and predicting the longitudinal shrinkage coefficients. Chalmers University of Technology was responsible for measuring the bow in the studs and the longitudinal shrinkage of the material, as well as for modeling bow.

The overall objective of this study was to predict the longitudinal shrinkage coefficient and bow of Norway spruce from color and tracheid effect data collected using nondestructive methods. The specific objectives of this study were to: measure bow at two moisture contents below the fiber saturation point; collect images of the stud surfaces using color scanning and tracheid effect scanning; cut the studs into smaller sticks and determine the longitudinal shrinkage coefficient for each stick; model the longitudinal shrinkage from the color and tracheid effect data; and model changes in the magnitude of bow for the two moisture contents.

Materials and methods

Materials

The selected material for this study was Norway spruce (*Picea abies*), which in Sweden is the principal material used in the building industry. Eight studs with a large variation in the amount of bow and compression wood content were selected for this study. Four of the studs were selected from a large study of moisture-related distortion. The results from the distortion study have been reported elsewhere by Johansson and Kliger⁵ and Johansson.⁹ The dimensions of the studs were 45 × 95 × 2500 mm (small studs). The material was dried in a kiln at conventional temperature (about 65°C) but without any outer restraint on the material. The other four studs came from logs with at least 25% visible compression wood at the butt end; they were selected at a sawmill. The studs measured 45 × 120 × 3000 mm (large studs). These studs were kiln-dried at conventional temperature (about 75°C) on top of a stack (i.e., without an outer restraint).

Distortion measurements

A device⁹ was developed to measure the distorted geometry every 5 cm along the length of the studs. The distortion was measured at two moisture contents below 18%. During the change in moisture content, each piece of timber was hung vertically in a conditioning room under ambient conditions. The purpose of hanging the timber vertically was to maximize the surface exposed to the air and eliminate any outer constraints on the material.

Scanning

After measuring the distortion, the studs were split into three slices 11 mm thick. The two outer slices were scanned on both sides, resulting in color and tracheid effect images. The middle slice was not scanned, but its surfaces were considered equal to the inner surfaces of the outer slices as just a saw kerf (1.5 mm) separated them.

Color

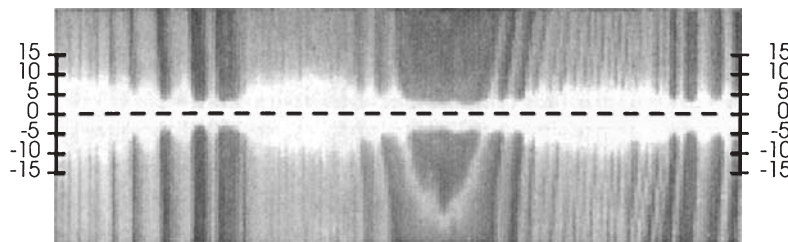
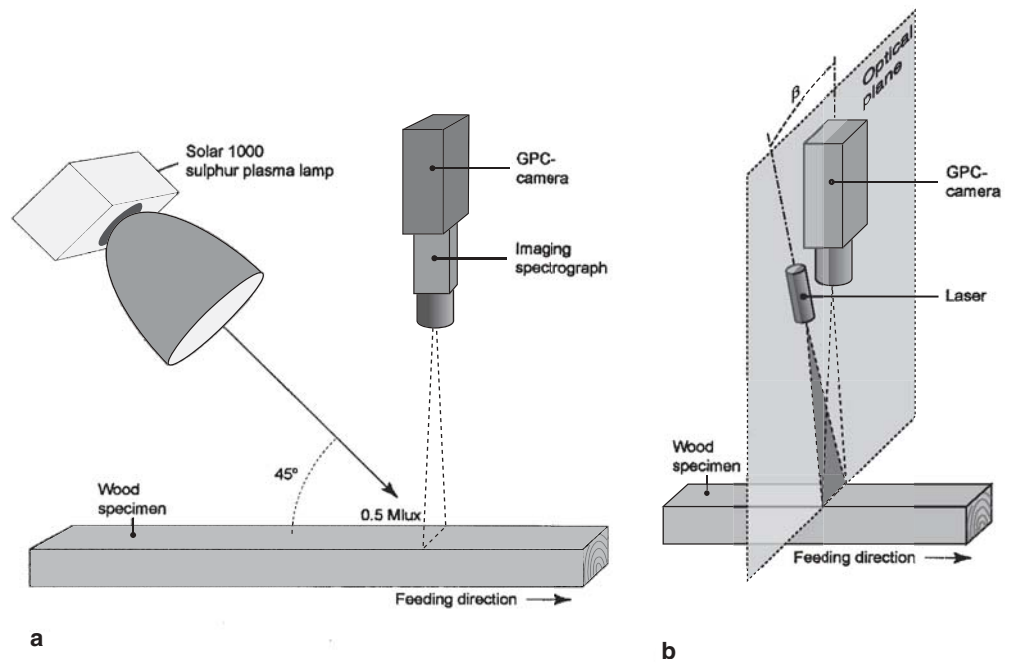
An imaging spectrometer was used to obtain color information from the wood surfaces, but the spectral information was converted to RGB color to reduce the number of variables used for modeling. The color scanning system used a camera equipped with an MAPP2200 (IVP AB, Linköping, Sweden) gray-scale matrix sensor combined with an imaging spectrograph (Specim, Oulu, Finland) (Fig. 1a). The system has a spectral resolution of 256 wavelength bands, which covers the visual spectrum; a detailed description of this system can be found in papers by Nyström and Hagman¹⁵ and Åstrand.²¹ The conversion from multispectral data to RGB color was made by averaging 20 spectral bands in the RGB region. This method simulates the output from an RGB color line scan camera.

Tracheid effect

The tracheid effect is the ability of a wood surface to conduct light in the direction of the fibers (Fig. 2). Wood fibers with special properties (e.g., compression wood and juvenile wood) have reduced light-conducting properties.

The scanning equipment consists of a gray-scale matrix camera with a “smart sensor” (the same as that used for color scanning) and a 670 nm, 30 mW diode laser with line generating optics (Lasiris; StockerYale, Salem, NH, USA). The laser was mounted on the side of the camera, aligned in such a way that the optical plane of the laser cuts through one specific sensor row in the middle of the sensor matrix, making the method independent of the distance to the object (Fig. 1b). Six tracheid images were then produced by integrating the intensity of reflected light at different distances from the laser line center. Integrating coefficients for the different classes, shown in Fig. 2, were implemented by controlling the exposure time for the corresponding sensor rows. The number and level of the integrating coefficients

Fig. 1. Setup for scanners. **a** Color scanner. **b** Tracheid scanner



	-16	-15	-14	-13	-12	-11	-10	-9	-8	-7	-6	-5	-4	-3	-2	-1	0	1	2	3	4	5	6	7	8	9	10	11	12	13	14	15	16	
tr1																	3																	
tr2																8		8																
tr3															20				20															
tr4													40	40						40	40													
tr5										80	80	60										60	80	80										
tr6	100	100	100	100	100	100	100	100	100																	100	100	100	100	100	100	100	100	100

Fig. 2. Integration coefficients for sensor rows forming six tracheid effect images (*tr1* to *tr6*). The laser line was centered on the sensor row marked 0

for each class were adjusted to make all the images similar in total intensity.

Sawing

The three slices from each stud were sawn into small sticks 10 × 10 × 200mm. This resulted in a total of (8 × 12 × 3) 288 sticks from each of the small studs and (10 × 14 × 3) 420 sticks from each of the large studs (Fig. 3). The complete studs were sawn into sticks, resulting not only in clear wood sticks but also in sticks with knots and other anomalies. Because the length of the studs could not be divided evenly into 200mm long pieces, 40–80mm was removed from the ends of each stud.

Longitudinal shrinkage

The length and weight of each stick were measured when the sticks were conditioned to equilibrium moisture content at 90% relative humidity (RH) and 21°C and when they were conditioned at 30% RH and 21°C. The oven-dried weight of each stick was also recorded after 24h at 104°C. The longitudinal shrinkage was quantified by the shrinkage coefficient α_l , expressed as the shrinkage strain (percent) per percentage moisture content change, as shown in Eqs. (1) and (2). The measurement procedure was described by Bengtsson.¹¹

$$\epsilon_l = \frac{l_1 - l_2}{l_1} \cdot 100 (\%) \tag{1}$$

$$\alpha_l = \frac{\varepsilon_l}{u_1 - u_2} \quad (\%/ \%) \quad (2)$$

where ε_l is the shrinkage strain; l_1 is the length at 90% RH; l_2 is the length at 30% RH; α_l is the longitudinal shrinkage coefficient; u_1 is the moisture content at 90% RH; and u_2 is the moisture content at 30% RH. The longitudinal shrinkage in spruce wood varies almost linearly with the moisture content,²² and it is reversible through several moisture cycles¹¹ below the fiber saturation point.

As all the material in each stud was sawn into sticks, it was unavoidable that some sticks had knots. In some cases, these knots were so large the stick were broken, and the longitudinal shrinkage coefficient could not be measured. Some of the sticks had a knot on one side or an uneven distribution of compression wood that led to the stick becoming bent during the change in moisture content, making it impossible to obtain a reliable value for the longitudinal shrinkage coefficient. In all, it was possible to measure the longitudinal shrinkage coefficient in 2473 sticks.

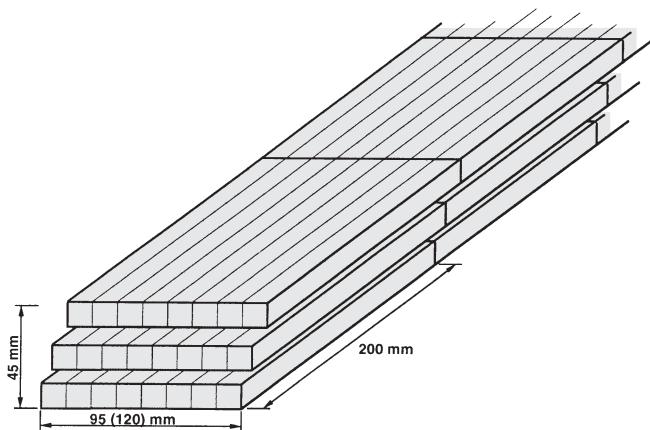
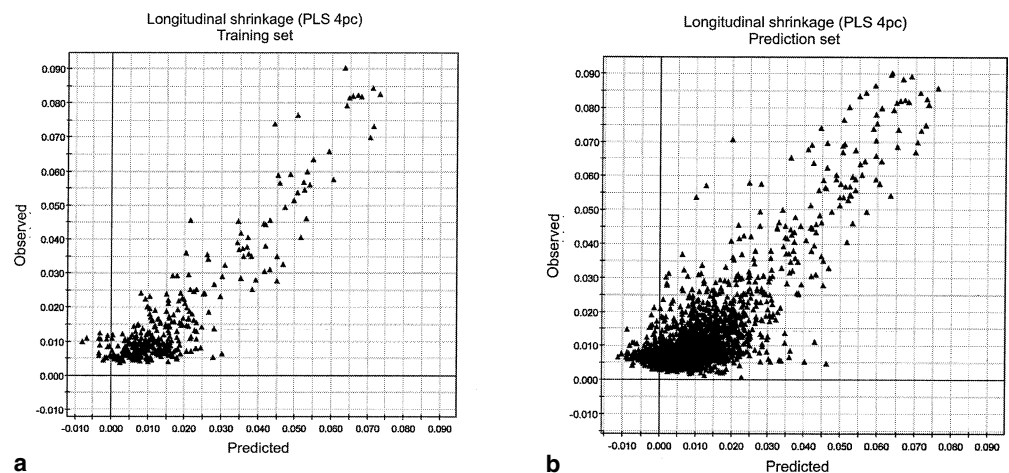


Fig. 3. Stud, slices, and sticks sawn from the stud

Fig. 4. Observed versus predicted longitudinal shrinkage coefficients for (a) the training set ($R^2 = 0.81$, RMSEP = 0.0071) and (b) the prediction set (RMSEP = 0.0079)



Multivariate modeling of longitudinal shrinkage coefficient

A total of nine variables were used in the data set for modeling the longitudinal shrinkage coefficient: six from tracheid effect measurements at various distances from the laser line (Fig. 2, tr1–tr6) and three color variables from the RGB wavelength bands. The scanned images had to be averaged to describe each corresponding stick sawn from the studs with one value per variable. Each stick was scanned on two opposite sides, so an average of the two sides was used for all the variables in the data set.

The model was trained using only part of the material (training set); the rest of the material (prediction set) was used for validation. Using an external prediction set is an effective way to validate the predictability of a model. Modeling was done using Simca-P 9.0 software for multivariate data analysis (Umetrics, Umeå, Sweden). The method used for multivariate regression in this study was PLS (partial least squares projections to latent structures). The PLS algorithm iteratively fits several variables to a response with linear models.

Only 4 of the 24 stud slices were used as a training set for the model (407 observations excluding missing values). The complementary observations were used in the prediction set for validation (2066 observations excluding missing values). Predictability was calculated using root mean square error of prediction (RMSEP) (Eq. 3), the standard deviation of the predicted residuals (error).

$$\text{RMSEP} = \sqrt{\frac{\sum_i (\text{obs}_i - \text{pred}_i)^2}{n}} \quad (\%/ \%) \quad (3)$$

where i is the observation number, and n is the total number of observations. The unit for RMSEP is the same as for the predicted variable – in this case α_l , which is dimensionless.

Results

Measurement of longitudinal shrinkage coefficient

The longitudinal shrinkage coefficient was obtained for a change in moisture content from 17.5% to 7.8%. The results showed a large variation in the longitudinal shrinkage coefficient. The mean longitudinal shrinkage coefficient was

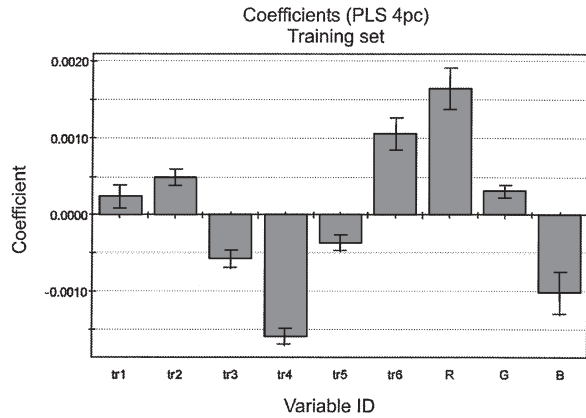


Fig. 5. Coefficients for all the variables in the PLS model. Variables with high coefficients (positive and negative) influence the model most. The 95% confidence interval is also marked

0.0121 (SD 0.0122). The longitudinal shrinkage coefficient ranged from 0.0008 to 0.0903, producing a factor of 113 ($0.0903/0.0008 = 113$) between the stick with the largest longitudinal shrinkage and the stick with the smallest longitudinal shrinkage (Table 1).

Modeling longitudinal shrinkage coefficient

The PLS model was based on the training set (4 of the 24 slices) with nine variables, six tracheid effect variables, and three color variables; the measured longitudinal shrinkage

Table 1. Longitudinal shrinkage coefficients for the sticks from each stud

Stud no.	No. of sticks	Mean (%/%)	SD (%/%)	Minimum (%/%)	Maximum (%/%)
1	259	0.0121	0.0079	0.0039	0.0573
2	272	0.0107	0.0056	0.0055	0.0324
5	236	0.0058	0.0011	0.0038	0.0113
6	273	0.0044	0.0019	0.0008	0.0208
3	391	0.0141	0.0076	0.0060	0.0501
4	359	0.0117	0.0098	0.0028	0.0740
7	338	0.0084	0.0056	0.0042	0.0536
8	345	0.0254	0.0232	0.0058	0.0903
Total	2473	0.0121	0.0123	0.0008	0.0903

The number of sticks, means, standard deviations, minimum and maximum longitudinal shrinkage coefficients are shown

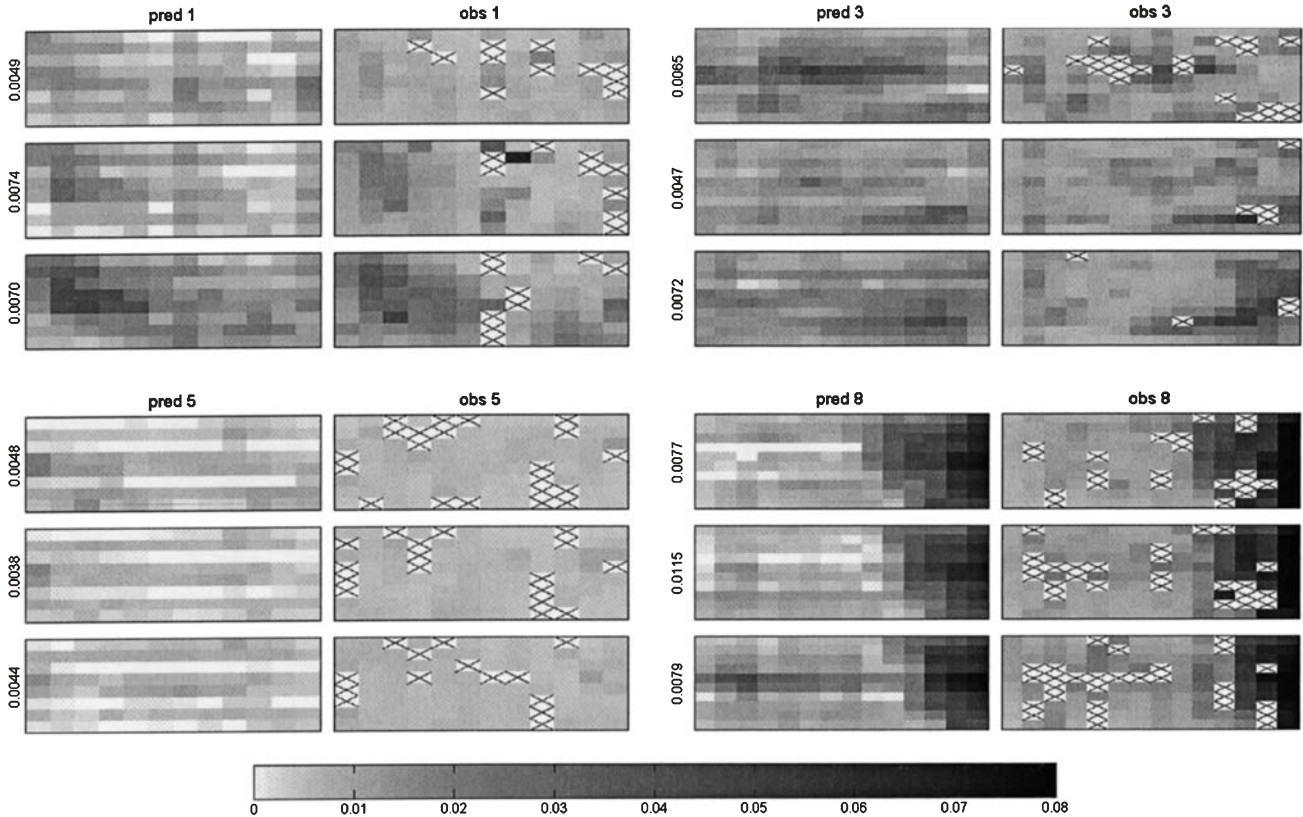
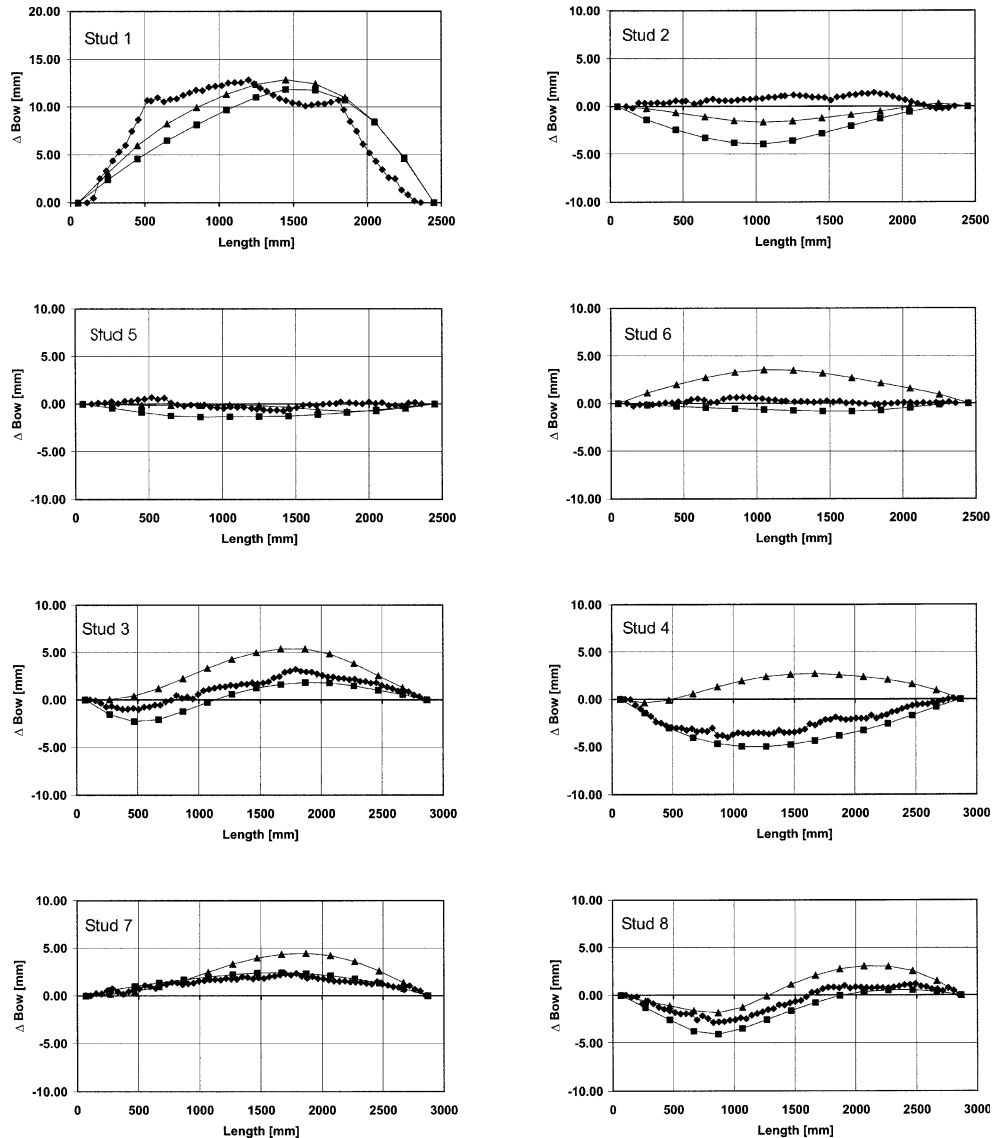


Fig. 6. Images of predicted (*pred*) and observed (*obs*) longitudinal shrinkage coefficient for four studs (nos. 1, 3, 5, 8). Each rectangle in the images represents one stick as seen from above (cf. Fig. 3). The darker the rectangle, the higher the longitudinal shrinkage measured

for that stick. The scale for the longitudinal shrinkage coefficient can be seen on the horizontal bar. The rectangles marked with a *cross* represent missing data. RMSEP values are shown to the left of each pair of slices

Fig. 7. Measured changes in bow (Δ Bow), Δ Bow calculated on the basis of the measured shrinkage data, and Δ Bow calculated on the basis of the predicted shrinkage data for all eight studs. Studs 1, 2, 5, and 6 measured $45 \times 95 \times 2500$ mm, and studs 3, 4, 7, and 8 measured $45 \times 120 \times 3000$ mm. Note that the scale for stud 1 has been shifted compared with the other scales. Triangles, Δ Bow based on predicted α_i ; squares, Δ Bow based on measured α_i ; diamonds, Measured Δ Bow



coefficient was the response variable. A model with four significant principal components and a coefficient of determination of $R^2 = 0.81$ was fitted. A plot of observed versus predicted values is shown in Fig. 4a. Some of the longitudinal shrinkage predictions are negative owing to the uncertainty of the model.

Predictability in terms of the RMSEP was 0.0071 for the training set. The coefficients and the confidence intervals for all the variables are shown in Fig. 5. The variables with the greatest influence on the model were the tracheid effect relatively far from the laser line (Fig. 2, tr4, tr6) together with red and blue color information.

Applying the PLS model to the prediction set produced an RMSEP of 0.0079, which is marginally larger than that of the training set. A plot of observed versus predicted values for the prediction set is shown in Fig. 4b. The mean predicted longitudinal shrinkage coefficient was 0.0113 (SD 0.0116).

The measured and predicted longitudinal shrinkage coefficients can be presented as images. They are compared, slice by slice, for some studs in Fig. 6. Missing data from the

observed images is likely to contain wood with large longitudinal shrinkage, as these sticks were deformed owing to the uneven distribution of compression wood or knots when the moisture content was lowered.

Modeling distortion

Bow and spring can be modeled on the basis of the variation in longitudinal shrinkage.⁹ This model was built up by joining 200 mm long distorted blocks to each other to form a complete stud. The distorted form of the blocks is calculated on the basis of the variation in longitudinal shrinkage over the block. The results showed that it was possible to model moisture-induced bow and spring fairly accurately based on the measured variation in longitudinal shrinkage.

The same model was used to predict changes in bow from the longitudinal shrinkage coefficients obtained from the PLS model. The change in bow in this case is called Δ Bow, which is the difference between the bow at a low

moisture content and the bow at a high moisture content. A compilation of the Δ Bow variation along the length of each stud is shown in Fig. 7. The measured Δ Bow, the Δ Bow calculated from the measured longitudinal shrinkage coefficient, and the Δ Bow calculated from the predicted longitudinal shrinkage coefficient are shown for each stud.

The results showed that the model produced reasonably accurate predictions for six of the eight studs. It was possible to model even curved Δ Bow and S-shaped Δ Bow. For seven of the eight studs, the Δ Bow modeled from the measured longitudinal shrinkage was more accurate than the Δ Bow modeled from the predicted longitudinal shrinkage. However, the results show that it is possible to model Δ Bow on the basis of data from images of the timber surface. It should be noted that not only the outer surfaces but also two inner surfaces were scanned.

Discussion

The results of this study show that it is possible to predict variations in the longitudinal shrinkage coefficient based on analysis of images of timber surfaces. The surfaces of the studs were scanned using two techniques: color scanning and tracheid effect scanning. The data from the images – three color variables from the RGB wavelength bands and six variables from the tracheid effect measurements at various distances from the laser line – were used to create a PLS (multivariate regression) model for the longitudinal shrinkage. The coefficient of determination between the measured and the predicted longitudinal shrinkage for the training set was 0.81. The RMSEP was used as a measure of the prediction. The RMSEP for the model was 0.0079, which is regarded as good. The mean value for the measured longitudinal shrinkage was 0.0121 (SD 0.0123). The mean predicted longitudinal shrinkage coefficient was 0.0113 (SD 0.0116).

The predicted longitudinal shrinkage coefficients were used to model changes in bow between two moisture contents below the fiber saturation point. The results showed that it was possible to model bow with reasonable accuracy. The results were almost as good as when the model was based on the measured longitudinal shrinkage. This shows that color and tracheid scanning is a possible method for predicting moisture-induced movements in bow for timber under the fiber saturation point.

Images of the wood surfaces were obtained at three levels through the thickness of the studs. By conducting the study in this way, it was possible to acquire knowledge of the three-dimensional variation in longitudinal shrinkage in the stud. For successful application of these techniques to industry, it is necessary to find out whether it is enough to know the variation in longitudinal shrinkage on the outer surfaces of the studs or if it is necessary to know the variation in longitudinal shrinkage within the stud.

If it is possible to model bow from images of the outer surfaces of timber, these techniques should make it possible to remove timber that become distorted before the timber

reaches its final end use. Removing this timber would make it possible to produce material with more predictable performance, an approach that would benefit the timber industry.

Acknowledgments The authors thank the European FAIR program (project “STUD” reg. no. CT 96-1915), the European Quality of Life program (project “Compression Wood” reg. no. QLRT-2000-00177), and the Swedish Foundation for Strategic Research (SSF) program (“Wood Technology”) for supporting this work.

References

- Johansson G, Kliger IR, Perstorper M (1994) Quality of structural timber: product specification system required by end-users. *Holz Roh Werkstoff* 52:42–48
- Eastin IL, Shook SR, Simon DD (1999) Softwood lumber substitution in the U.S. residential construction industry in 1994. *For Prod J* 49(5):21–27
- Eastin IL, Shook SR, Fleishman SJ (2001) Material substitution in the U.S. residential construction industry, 1994 versus 1998. *For Prod J* 51(9):30–37
- Johansson M, Perstorper M, Kliger R, Johansson G (2001) Distortion of Norway spruce timber. Part 2. Modelling twist. *Holz Roh Werkstoff* 59:155–162
- Johansson M, Kliger R (2002) Influence of material characteristics on warp in Norway spruce timber. *Wood Fiber Sci* 34:325–336
- Alhasani MA (1999) Growth stresses in Norway spruce. Report TVBK-1016. Lund Institute of Technology, Division of Structural Engineering, Lund, Sweden
- Archer RR (1987) Growth stresses and strains in trees. Springer, Berlin, p 240
- Stanish MA (2000) Predicting the crook stability of lumber within the hygroscopic range. *Drying Technol* 18:1879–1895
- Johansson M (2002) Moisture-induced distortion in Norway spruce timber – experiments and models. PhD thesis, Chalmers University of Technology, Gothenburg, Sweden
- Kliger R, Johansson M, Perstorper M (1997) Influence of three-dimensional variation in shrinkage on distortion. In: Proceedings of COST Action E8, International Conference on Wood-Water Relations, Copenhagen, pp 153–164
- Bengtsson C (2001) Variation of moisture induced movements in Norway spruce. *Ann For Sci* 58:569–581
- Zobel BJ, Sprague JR (1998) Juvenile wood in forest trees. Springer, Berlin, p 300
- Timell TE (1986) Compression wood in gymnosperms. Springer, Berlin, p 2190
- Perstorper M, Johansson M, Kliger R, Johansson G (2001) Distortion of Norway spruce timber. Part 1. Variation of relevant wood properties. *Holz Roh Werkstoff* 59:94–103
- Nyström J, Hagman O (1999) Real time spectral classification of compression wood in *Picea abies*. *J Wood Sci* 45:30–37
- Nyström J, Kline DE (2000) Automatic classification of compression wood in green Southern yellow pine. *Wood Fiber Sci* 32:301–310
- Nyström J (1999) Image based methods for nondestructive detection of compression wood in sawn timber. Licentiate thesis, Luleå University of Technology, p 34, ISSN: 1402–1757
- Nyström J (2003) Automatic measurement of fiber orientation in softwoods by using the tracheid effect. In: Computers and Electronics in Agriculture (in press)
- Seltman J (1992) Indication of slope-of-grain and biodegradation in wood with electromagnetic waves. In: Lindgren O (ed) Proceedings of the 1st international seminar on scanning technology and image processing on wood. Luleå University of Technology, Skellefteå Campus, Sweden
- Wendland G (2000) Beitrag zur automatischen Oberflächeninspektion von Holz anhand optischer Eigenschaften. PhD thesis, Technischen Universität Dresden, Germany
- Åstrand E (1996) Automatic inspection of sawn wood, PhD thesis no. 424, Linköping University, Sweden
- Skaar C (1988) Wood-water relations. Springer, Berlin, p 283